Changes in Stability upon Charge Reversal and Neutralization Substitution in Staphylococcal Nuclease Are Dominated by Favorable Electrostatic Effects†

Jeffery M. Schwehm,‡,§ Carolyn A. Fitch,|| Bao N. Dang,‡,⊥ Bertrand García-Moreno E.,|| and Wesley E. Stites*,‡

Department of Chemistry and Biochemistry, University of Arkansas, Fayetteville, Arkansas 72701-1201, and Department of Biophysics, The Johns Hopkins University, Baltimore, Maryland 21218

Received August 15, 2002; Revised Manuscript Received November 18, 2002

ABSTRACT: Single site mutations that reverse or neutralize a surface charge were made at 22 ionizable residues in staphylococcal nuclease. Unfolding free energies were obtained by guanidine hydrochloride denaturation. These data, in conjunction with previously obtained stabilities of the corresponding alanine mutants, unequivocally show that the dominant contribution to stability for virtually all of the wild-type side chains examined is the electrostatic effect associated with each residue's charged group. With only a few exceptions, these charges stabilize the native state, with an average loss of 0.5 kcal/mol of stability upon neutralization of a charge. When the charge is reversed, the average destabilization is doubled. Structure-based calculations of electrostatic free energy with the continuum method based on the finite difference solution to the linearized Poisson−Boltzmann equation reproduce the observed energetics when the polarizability in the protein interior is represented with a dielectric constant of 20. However, in some cases, large differences are found, giving insight into possible areas for improvement of the calculations. In particular, it appears that the assumptions made in the calculations about the absence of electrostatic interactions in the denatured state and the energetic consequences of dynamic fluctuations in the native state will have to be further explored.

It is widely recognized that electrostatic interactions contribute to the stability of proteins. This is evident from the fact that the stability of most proteins is highly sensitive to pH, as well as from a variety of studies in which surface-ionizable residues were perturbed by mutagenesis and the consequences on stability measured experimentally. Unfortunately, it has been difficult to define the general trends in the character and magnitude of electrostatic contributions to stability. For example, short-range Coulombic interactions can contribute significantly to the stability of the native state (*1*). In some cases, buried ion pairs have been found to contribute as much as 2−5 kcal/mol (*2*). However, the contributions by electrostatic interactions to protein stability in general tend to be modest. In fact, there are numerous examples where the electrostatic contribution to stability is less than 1 kcal/mol, even for residues interacting at short ranges (*3*−*10*).

Structure-based calculations with continuum methods have influenced significantly our understanding of the character of electrostatic effects in proteins. They have promoted the notion that electrostatic contributions to protein stability are large. However, until recently, the calculated energies of Coulombic interactions between surface charges were exaggerated and significantly greater than the measured energies (*11*, *12*). For example, in the case of myoglobin, large stabilizing contributions >1 kcal/mol were calculated for ion-paired residues (*13*), yet the observed energies were <0.5 kcal/mol (*14*). The calculation of energies of interaction between ion-paired residues is particularly difficult because the interacting charges interfere with each other's hydration layer; thus, in addition to the Coulombic contribution, it is also necessary to quantitate hydration energies.

To improve the agreement between calculated and measured electrostatic energies, empirical methods have been developed (*11*, *15*) that reduce the magnitude of calculated electrostatic potentials by increasing the apparent polarizability of the protein. This can be achieved directly, through the use of arbitrarily high dielectric constants, or indirectly, by accounting explicitly for the consequences of conformational flexibility that are not implicit in the protein dielectric constants. It is noteworthy that even with these empirical adjustments the calculations still predict that most surface-charged groups are in electrostatically favorable environments. This is consistent with the experimental observation that most pK_a values of ionizable residues in proteins are shifted in the direction that signals net favorable electrostatic influences.

One of the significant disagreements that has existed between calculated and measured electrostatic free energies concerned the magnitude of long-range Coulombic interactions and their contributions to stability. According to calculations with static structures using the continuum method based on the finite difference solution of the Poisson−

† This work was supported by NIH Grants GM 52714 and NCRR COBRE 1 P20 RR15569 (W.E.S.) and NSF Grant MCB-9600991 (B.G.-M.,E.).

* To whom correspondence should be addressed. Phone: 479-575-7478. Fax: 479-575-4049. E-mail: wstites@uark.edu.

‡ University of Arkansas.

§ Present address: Department of Natural Sciences, Concordia University, 800 N. Columbia Ave., Seward, NE 68434.

|| The Johns Hopkins University.

⊥ Present address: Family Medical Care, 7600 S. Lewis, Tulsa, OK 74136.

10.1021/bi0266434 CCC: $25.00 © 2003 American Chemical Society
Published on Web 01/03/2003

Boltzmann equation (FDPB),[1] medium- and long-range electrostatic interactions are strong, and they contribute significantly to the stability of proteins. In contrast, long-range electrostatic interactions measured experimentally in T4 lysozyme are extremely weak (*4*). Recently, it was demonstrated experimentally that although long- and medium-range pairwise Coulombic interactions are weak, many such interactions can in aggregate produce substantial electrostatic effects (*9*, *10*). This explains why it has been possible to increase the stability of proteins significantly by judicious alteration of the pattern of medium- and long-range attractive and repulsive interactions (*16*−*18*).

Although reports abound where the energetic contribution of a few ionizable residues is examined, surprisingly, to the best of our knowledge, there is only one study in which the energetic contribution of a large number of such residues was systematically examined. In that particular study of staphylococcal nuclease, all of the ionizable side chains (23 lysines, 5, arginines, 4 histidines, 12 glutamates, and 8 aspartates) were substituted with alanine (*19*). The study concluded that electrostatic interactions of the ionizable amino acids in staphylococcal nuclease made only a small contribution to the net stability of the protein. This important study has one shortcoming with regard to specifically assessing electrostatic contributions. Truncating the side chain of an ionizable residue by substituting an alanine removes not only electrostatic interactions but also van der Waals interactions. It eliminates the possibility for hydrophobic interactions with the methylene units of the side chains and possibly alters the degrees of freedom of the side chain in the denatured state significantly. Indeed, it was concluded that the ionizable amino acids in staphylococcal nuclease contributed to the stability of the native state mainly through packing and other interactions that do not depend on the charge of the amino acid side chain. This conclusion was supported to some degree by the results of a more recent study where the stability effects of increasing the hydrophobicity of amino acids on the surface of nuclease were measured (*20*). That study also concluded that packing interactions on the surface of globular proteins are important to protein stability.

A strategy better suited for determining the contribution of electrostatic interactions to protein stability is to substitute the ionizable side chains with oppositely charged residues (charge reversal substitutions) and neutral, polar residues (charge neutralization substitutions). Such substitutions are much more conservative in size and shape than a truncation to alanine. While this approach has been previously used, again rather surprisingly, a systematic examination of such mutants has not been undertaken. The largest data sets of such substitutions of which we are aware are six charge reversal mutations in T4 lysozyme (*21*) and six charge neutralization mutations in human lysozyme (*22*).

A larger data set is needed to identify the general trends and the patterns in the contributions by surface-charged residues to protein stability. Therefore, six glutamates were mutated to lysine and glutamine, four aspartates were mutated to asparagine and lysine, nine lysines were mutated to glutamine and glutamate, and one histidine was mutated to glutamate and glutamine in the model protein staphylococcal nuclease. Structure-based electrostatic free energy calculations using the FDPB continuum method were performed both to interpret the measured energetics and to test the ability of these methods to reproduce the experimental data. This study provides novel insights into the magnitude and character of electrostatic contributions to stability, which will improve our ability to engineer the stability in proteins by replacement of medium- and long-range repulsive interactions with attractive interactions, as demonstrated recently by others (*16*−*18*).

MATERIALS AND METHODS

Mutagenesis, Protein Expression, Protein Purification, and Guanidine Hydrochloride Denaturations. The mutants were prepared by the method of Kunkel (*23*, *24*) as described previously. Protein expression and purification were performed as previously described (*20*). Guanidine hydrochloride denaturations were performed in 100 mM sodium chloride and 25 mM sodium phosphate, pH 7, using an Aviv model ATF-101 fluorometer as previously described (*25*, *26*). Briefly, the apparent equilibrium constant is calculated from the relative fluorescence intensity, I, at each data point along the denaturation curve using the equation $K_{app} = (I_N - I)/(I - I_D)$, where I_N and I_D are the intensities of the native baseline and denatured baseline, respectively. Both baselines of staphylococcal nuclease mutants are usually flat or very nearly so (as were all of the mutants here). In the event that the protein was destabilized enough that a native baseline was not available, a linear dependence of log K_{app} on guanidine hydrochloride concentration was assumed and the value of I_N was iteratively modified until a stable value was found. None of the mutants used in this study were sufficiently destabilized to require ammonium sulfate renaturation.

Calculations. The Protein Data Bank accession code for the wild-type structure used in calculations is 1STN (*27*). Structures for the alanine mutants were generated by truncating the residue to the β carbon. Charge neutralization and charge reversal mutants were constructed within the InsightII software package (Accelerys Inc.). Mutated side chains were energy minimized beginning with the γ carbon and including all polar hydrogens. Five charge reversal mutants, D19K, E135K, E5K, E10K, and E67K, were found to be extremely destabilized unless the lysine side chain was rotated about the $C_\alpha-C_\beta$ bond to maximize the side chain's interaction with solvent.

Electrostatic free energies of the mutants and wild-type structures were calculated using the continuum method based on the solution of the linear Poisson−Boltzmann equation, using the single site ionization protocol described previously by Antosiewicz et al. (*11*, *12*). The cluster method was used in the calculation of the ionization energetics (*28*). Finite difference Poisson−Boltzmann (FDPB) calculations were performed with the University of Houston Brownian Dynamics package (*29*). Polar hydrogens were added to the crystallographic structure (1STN), using the HBUILD facility of CHARMm version 25.2 (Accelrys Inc.). Hydrogen atoms were placed on Oδ2 of all aspartic acid residues and on Oϵ2 of all glutamic acid residues. Histidine tautomeric forms were determined by the best fit to experimental pK_a values of wild-

[1] Abbreviation: FDPB, finite difference Poisson−Boltzmann.

type staphylococcal nuclease as described previously (*9*, *10*). Therefore, hydrogens were placed on His-8 Nϵ2, His-46 Nδ1, His-121 Nϵ2, and His-124 Nδ1 for all calculations. Initial positions of added hydrogens were energy minimized in CHARMm using 500 steps of steepest descent. Partial charges were taken from the CHARMm polar hydrogens only topology file version 21. Atomic radii were taken from the OPLS parameter set (*30*). The following set of titratable sites and model compound pK_a values was used: C-terminus main chain C, 3.8; Asp Cγ, 4.0; Glu Cδ, 4.4; His Nδ1 or Nϵ2, 6.3; N-terminus main chain N, 7.5; Tyr OH, 9.6; Lys Nζ, 10.4; Arg Cζ, 12.0. The following parameters were held constant in all calculations unless noted otherwise: temperature, 298 K; ionic strength, 125 mM; protein dielectric constant, 20.0; water dielectric constant, 78.5; Stern layer, 2.0 Å. Richard's probe-accessible surface (*31*) was calculated with a probe radius of 1.4 Å. Under the conditions used in the calculations all ionizable groups are fully charged except tyrosines and histidines.

The calculated shift in electrostatic energy of the mutant from the wild-type protein, G_{elec}, was calculated as for the experimental data, by subtraction of the unfolding free energy, G_{elec}, calculated at pH 7 for the mutant from that of wild type. All calculations assume a noninteracting random coil for the denatured state.

RESULTS

A total of 22 charge neutralization and 20 charge reversal substitutions were made at 22 sites in staphylococcal nuclease. Of these 22 sites chosen, 10 were lysines, 7 were glutamates, 4 were aspartates, and 1 was a histidine. Of the 10 lysines, 9 were substituted with glutamate and glutamine. At site K133, only the glutamine substitution was successfully made. Of the 7 glutamates, 6 were substituted with glutamine and lysine. At site E67, only the glutamine substitution was obtained. The aspartate sites were substituted to asparagine and lysine, and the histidine site was substituted to lysine and glutamine. No known previous mutation of staphylococcal nuclease has caused great perturbation of the overall structure. We have solved crystal structures of staphylococcal nuclease mutants with buried ionizable residues (*32*, *33*), and even in such extreme cases the overall fold of the protein is unchanged. The identities of the mutants and the stability parameters derived from guanidine hydrochloride denaturations are found in Table 1.

Guanidine hydrochloride denaturation was used to determine the stability difference between the denatured and native states. Representative denaturation curves are shown in Figure 1. Use of guanidine hydrochloride is validated by the previous demonstration that the ionic strength dependence of histidine pK_a values in nuclease is linear in the range 0.01−1.0 M (*9*). The ionic strength effects inherent to guanidine hydrochloride are corrected by the linear extrapolation used to obtain free energies. The use of the nonionic denaturant, urea, has been the subject of preliminary investigations. Urea solutions are usually made up fresh every day because of isocyanate formation, and because of the relatively low denaturing power of urea large dilutions are required in a titrating instrument such as ours. Unfortunately, perhaps because of these factors, the reproducibility of these urea denaturation curves has thus far been relatively poor compared to guanidine hydrochloride. It should be noted that the values from urea denaturation that are in hand do not agree particularly well with the guanidine hydrochloride denaturation parameters. It is not uncommon for proteins to have different apparent stabilities found upon urea and guanidine hydrochloride denaturation (*34*−*39*). This is frequently attributed to the ionic character of guanidine hydrochloride (*40*, *41*), but not always (*42*). Reports of different degrees of residual structure in the unfolded state(s) generated by the two denaturants are also common (*43*−*47*). However, urea denaturation of the mutants here apparently shows nearly half to have stability greater than that of wild type, often by 1 kcal/mol or more. Given that mutations in

Table 1: Guanidine Hydrochloride Denaturation Parameters for Charge Reversal and Charge Neutralization Substitutions in Staphylococcal Nuclease

mutant	m_{GuHCl}[a]	C_m[b]	ΔG_{H_2O}[c]	mutant	m_{GuHCl}[a]	C_m[b]	ΔG_{H_2O}[c]
E10K	5.81	0.55	3.2	E75Q	6.27	0.74	4.7
E10Q	5.74	0.72	4.1	D77K	5.54	0.35	1.9
D19K	6.93	0.74	5.1	D77N	5.74	0.44	2.5
D19N	5.94	0.87	5.2	K78E	6.27	0.73	4.6
D21K	6.34	1.02	6.4	K78Q	6.67	0.79	5.3
D21N	6.47	1.05	6.8	K84E	6.60	0.82	5.4
K28E	6.53	0.70	4.6	K84Q	6.73	0.79	5.3
K28Q	6.53	0.78	5.1	K97E	6.20	0.77	4.8
K48E	6.34	0.85	5.4	K97Q	6.34	0.79	5.0
K48Q	6.47	0.83	5.3	E122K	5.87	0.46	2.7
E57K	6.27	0.84	5.3	E122Q	6.20	0.60	3.8
E57Q	6.34	0.81	5.2	H124E	6.07	0.93	5.6
K63E	6.60	0.60	3.9	H124Q	6.40	0.94	6.0
K63Q	6.20	0.70	4.4	K127E	6.34	0.86	5.4
K64E	7.00	0.55	3.8	K127Q	6.40	0.84	5.4
K64Q	6.53	0.82	5.4	K133Q	6.53	0.76	4.9
E67Q	6.80	0.72	4.9	E135K	6.80	0.63	4.3
K70E	6.34	0.79	5.0	E135Q	6.60	0.71	4.7
K70Q	6.47	0.79	5.1	D143K	6.47	0.78	5.1
E73K	6.60	0.51	3.3	D143N	6.34	0.80	5.1
E73Q	6.47	0.73	4.7	wild type	6.53	0.82	5.4
E75K	6.27	0.49	3.1				

[a] Slope value (change in free energy with respect to change in guanidine hydrochloride concentration). Units of kcal/(mol·M). Error is estimated to be ±0.09. [b] Concentration of guanidine hydrochloride at the midpoint of denaturation expressed in molarity. Error is estimated to be ±0.01 M. [c] The free energy difference between the native and denatured states at zero guanidine hydrochloride concentration expressed in kcal/mol. Error is estimated to be ±0.1 kcal/mol.

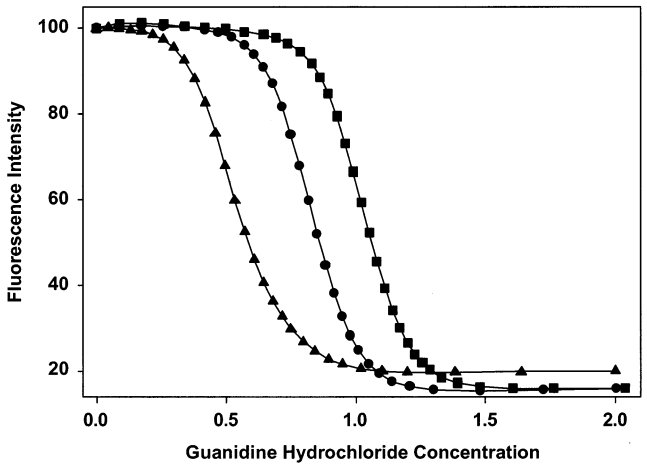

FIGURE 1: Relative fluorescence intensity versus guanidine hydrochloride concentration for representative proteins: wild-type staphylococcal nuclease (circles), D21K (squares), and E10K (triangles). The intensity of the first point is arbitrarily set to 100.

Table 2: Solvent Accessibility, Secondary Structure, Ion Pairs, Hydrogen Bonding, and Relative Stabilities of Alanine, Charge Neutralization, and Charge Reversal Substitutions

site	SASA[a]	sec struct[b]	ion pairs[c]	H-bond[d]	$\Delta\Delta G_{A\rightarrow WT}$[e]	$\Delta\Delta G_{NU\rightarrow WT}$[f]	$\Delta\Delta G_{RV\rightarrow WT}$[g]	$\Delta\Delta G_{NU\rightarrow RV}$[h]
E10	0.20	E	K28, R81	Y27	1.2	1.3	2.2	0.9
D19	0.09	S	K45, K16, R87, R35	T44	0.0	0.2	0.3	0.1
D21	0.02	S	R35, *K45*, *R87*	T22, T44	−0.8	−1.4	−1.0	0.4
K28	1.03	T	E10	Y27	0.6	0.3	0.8	0.5
K48	1.28	T			−0.2	0.1	0.0	0.5
E57	0.56	H	K53		0.1	0.2	0.1	−0.1
K63	0.74	H	E67		0.4	1.0	1.5	0.4
K64	1.15	H	E67		−0.2	0.0	1.6	1.6
E67	0.36	H	K63, *K16*, *K64*		0.9	0.5	n/d[i]	n/d[i]
K70	1.06	S	D95		0.0	0.3	0.4	0.1
E73	0.20	E	K71, K9		1.3	0.7	2.1	1.4
E75	0.00	E	K9	Y93	2.1	0.7	2.3	1.6
D77	0.00	N	*K78*, *R81*	Y91, T120	3.0	2.9	3.5	0.8
K78	0.69	S	D77	T120	0.5	0.1	0.8	0.7
K84	1.08	T	D83	Y85	−0.3	0.1	0.0	−0.6
K97	1.05	E	K78, *D95*, *E101*		0.0	0.4	0.6	0.2
E122	0.09	H	R126, *K116*		0.3	1.6	2.7	1.1
H124	0.64	H			−0.5	−0.6	−0.2	0.4
K127	1.04	H			−0.3	0.0	0.0	0.0
K133	0.55	H	E129		1.3	0.5	n/d[i]	n/d[i]
E135	0.44	T	R105, K134		0.6	0.7	1.1	0.4
D143	n/a[j]	n/a[j]	n/a[j]		0.0	0.3	0.3	0.0

[a] Fraction of the solvent-accessible surface area of the wild-type side chain relative to the surface area of that side chain in an Ala-Xxx-Ala tripeptide in extended conformation. [b] Secondary structure determination by the method of Kabsch and Saunders (*48*): E, β-sheet; H, α-helix; S, bend; T, hydrogen-bonded turn; N, no regular secondary structure. [c] Side chains involved in ion pairs in the wild-type protein. Normal script is used for side chains in an ion pair separated by less than 5 Å. Italics is used for side chains whose ion pair partner is between 5 and 10 Å away (*10*). Both structures 1STN and 1EYO were examined (*27*, *49*). [d] The side chains of the neutral polar residues listed in this column are hydrogen-bonding partners (distance of not less than 5 Å to the polar atom) with the ionizable side chain. [e] The difference in stability of the wild-type protein (ΔG_{WT} = 5.4 kcal/mol) and the stability of the respective alanine substitutions where $\Delta\Delta G_{A\rightarrow WT} = \Delta G_{WT} - \Delta G_{Ala}$. ΔG_{Ala} values are taken from Meeker et al. (*19*). [f] The difference in stability of the wild-type protein (ΔG_{WT} = 5.4 kcal/mol) and the stability of the respective charge neutralization substitutions where $\Delta\Delta G_{NU\rightarrow WT} = \Delta G_{WT} - \Delta G_{NU}$. [g] The difference in stability of the wild-type protein (ΔG_{WT} = 5.4 kcal/mol) and the stability of the respective charge reversal substitutions where $\Delta\Delta G_{RV\rightarrow WT} = \Delta G_{WT} - \Delta G_{RV}$. [h] The difference in stability in kcal/mol between the single site charge reversal substitutions and their corresponding single site charge neutralization substitutions where $\Delta\Delta G_{NU\rightarrow RV} = \Delta G_{RV} - \Delta G_{NU}$. [i] Not determined. [j] Not applicable. Residues 142−149 are disordered in the X-ray structure so these parameters are undefined.

staphylococcal nuclease and all other proteins are almost always destabilizing, and also given the good agreement between theory and the guanidine hydrochloride data discussed later in this publication, we suspect that our urea denaturation numbers are not accurate. We are working to understand the source of this discrepancy and expect that data based on urea denaturation will form the basis of future publications. We are confident in the guanidine hydrochloride data presented here, but it is appropriate that the issue of possible ionic strength dependence be remembered as a potential source of error in any interpretation.

The average loss in stability for all of the charge neutralization substitutions is 0.5 kcal/mol with a standard deviation of 0.8 kcal/mol. In a previous study (*19*), all ionizable residues were substituted with alanine. The average stability loss for the alanine substitutions at the positions where charge reversal or neutralization mutation was carried out is 0.5 ± 0.9 kcal/mol. Interestingly, the average stability loss for all of the charge reversal substitutions is 1.0 ± 1.1 kcal/mol, about twice that of charge neutralization. The changes in stability relative to wild type for the alanine, charge neutralization, and charge reversal substitutions for the individual sites are shown in Table 2 along with a summary of some structural data for each site (*48*, *49*).

Staphylococcal nuclease has a rather high net positive charge of 9 at pH 7, as befits an enzyme with high affinity for nucleic acids. It is therefore not surprising that the neutralization of a negative charge costs on average 0.7 ± 0.9 kcal/mol and reversing it to a positive charge costs 1.4 ± 1.3 kcal/mol. Although pairwise, medium-range, and long-range Coulombic interactions in nuclease are very weak (*10*), this shows that many individual interactions can in aggregate produce a substantial effect. This is confirmed by the interesting observation that even the positively charged side chains are usually in stabilizing electrostatic environments, albeit less so, with neutralization costing 0.3 ± 0.4 kcal/mol and substitution with a negatively charged side chain costing 0.6 ± 0.6 kcal/mol on average.

The electrostatic free energies calculated with the FDPB method are shown in Table 3 ($\Delta\Delta G_{elec}$). The subscript elec is used to emphasize that these calculated energies include *only* the electrostatic component. On average the calculated stability loss for the alanine substitutions was 0.1 ± 0.7 kcal/mol. The average loss of stability for all charge neutralization substitutions is 0.3 ± 0.07 kcal/mol, and for charge reversal substitutions it is 1.25 ± 1.37 kcal/mol. The calculated $\Delta\Delta G_{elec}$ values were dissected further into contributions from Coulombic interactions, from interactions with permanent dipoles, and from differences in hydration in the native state and in a fully hydrated denatured state. The net electrostatic consequences calculated for most mutations are destabilizing. This reflects a balance between contributions with opposite signs. The Born terms, due to the difference in the state of hydration of an ionizable group in the native and in the denatured state, are unfavorable for most residues in the native state of the wild-type protein. Thus the calculated Born energies stabilize the mutants where charge is removed. In

Table 3: Calculated Changes in Stability of Charge Neutralization and Charge Reversal Substitutions Using the FDPB Method

mutant	$\Delta\Delta G_{elec\ Ala\rightarrow WT}$[a]	$\Delta\Delta G_{elec\ RV\rightarrow WT}$[b]	$\Delta\Delta G_{elec\ NU\rightarrow WT}$[c]
E10	0.6	1.38	0.49
D19	−0.36	1.30	−0.48
D21	−1.58	0.31	−0.94
K28	0.11	1.06	0.48
K48	−0.2	−0.33	−0.02
E57	0.8	1.38	0.72
K63	0.57	1.74	0.77
K64	0.19	0.84	0.36
E67	1.22	2.23	1.77
K70	−0.16	0.33	−0.01
E73	0.24	2.2	0.18
E75	0.59	3.47	1.00
D77	0.43	4.40	0.38
K78	−0.5	1.17	−0.2
K84	−1.13	−0.95	−0.93
K97	0.3	1.34	0.47
E122	0.86	3.07	1.50
H124	−0.22	0.06	0.22
K127	−0.53	−0.65	−0.39
K133	0.36	1.78	0.83
E135	1.27	1.93	1.27

[a] The calculated difference in stability in kcal/mol between wild-type nuclease and the alanine substitutions where $\Delta\Delta G_{elec\ Ala\rightarrow WT} = \Delta G_{elec\ WT} - \Delta G_{elec\ Ala}$. The subscript elec is used to emphasize that these calculated energies include *only* an electrostatic component. [b] The calculated difference in stability between wild-type and the charge reversal substitutions where $\Delta\Delta G_{elec\ RV\rightarrow WT} = \Delta G_{elec\ WT} - \Delta G_{elec\ RV}$. [c] The calculated difference in stability between wild-type and the charge reversal substitutions where $\Delta\Delta G_{elec\ NU\rightarrow WT} = \Delta G_{elec\ WT} - \Delta G_{elec\ NU}$.

contrast, the terms that describe interactions with other charged groups or with permanent dipoles are always stabilizing in the native state of the wild-type protein. The net destabilizing consequence of mutations means that the Coulombic and permanent dipole terms outweigh the Born term in most cases. Not only did the FDPB method reproduce the direction of the shift in stability for most mutants correctly, it also reproduced the magnitude of the shift remarkably well. The root mean squares of the differences of the calculated and the observed stability shifts are 0.91, 0.79, and 0.66 kcal/mol for the alanine, charge neutralization, and charge reversal substitutions.

A second pK_a calculation using the FDPB method was performed to assess the sensitivity of our results to the details of the calculation and to ensure that the conclusions drawn from the calculations were robust. In this second calculation a distributed charge model was used to describe the ionized state (*12*), the van der Waals surface was used to define the dielectric boundary, and the protein interior was treated with a dielectric constant of 4. This method has been shown to reproduce experimental results very accurately in other cases (*50*, *51*). The results of this second calculation are not presented because, in general, the $\Delta\Delta G_{elec}$ values calculated with the two methods are comparable to the values that are presented in Table 3. In almost every case the magnitudes of the $\Delta\Delta G_{elec}$ calculated with the method using the distributed charge model and the van der Waals surface are greater than the values calculated with the single site method and the solvent-accessible surface. In a few specific cases there are significant differences in the $\Delta\Delta G_{elec}$ calculated with the two methods; however, the trends are comparable. The correlation between experimental and calculated $\Delta\Delta G_{elec}$ values calculated by the two methods are also comparable, and the conclusions drawn from the calculated values are independent of the details of the method used to calculate $\Delta\Delta G_{elec}$.

DISCUSSION

How energetically important are electrostatic interactions relative to other types of noncovalent interactions of surface ionizable residues? Twenty-two ionizable residues in staphylococcal nuclease were chosen for this study. These sites, about half of all ionizable residues in nuclease, were chosen to cover a range of solvent accessibility, secondary structure, and side chain hydrogen bonding. In this way, a broad sampling of electrostatic interactions in different structural contexts could be assessed.

Our strategy for determining the contributions of electrostatic interactions to protein stability was to substitute the ionizable side chains at selected sites in staphylococcal nuclease with oppositely charged residues (charge reversal substitutions) and neutral, polar residues (charge neutralization substitutions). Accordingly, glutamic acid residues were substituted with glutamine and lysine, and aspartic acids were substituted with asparagine and lysine. Lysine and histidine were substituted with glutamate and glutamine. In previously published work all of these sites have been substituted with alanine (*19*), and many have been substituted with phenylalanine (*20*).

Substitution of a side chain always changes a variety of noncovalent interactions (e.g., changes in hydrophobicity, van der Waals interactions, side chain entropy), not just electrostatic interactions. The conservative substitutions made here minimize these problems as much as possible. On the other hand, truncation to an alanine maximizes these other effects, removing not only all electrostatic interactions but all other stabilizing or destabilizing interactions beyond the β carbon. Therefore, comparison to the stabilities of the alanine substitutions can help us to estimate how sensitive a given site is to other effects.

The effects of charge neutralization and reversal are compared with the effects of alanine substitution in Figure 2. First we consider the comparison of the effects of charge neutralization substitutions and the alanine substitutions, shown in Figure 2A. Generally speaking, the charge neutralization substitution (i.e., replacement with a glutamine or asparagine) is the most conservative substitution possible. It conserves hydrophobic and/or van der Waals interactions of the methylenes in the side chain, extremely well in the case of glutamate or aspartate and fairly well for lysine. The amide moiety retains capacity for hydrogen-bonding interactions but eliminates Coulombic interactions between formal charges. An alanine substitution removes all of the interactions of the side chain.

The dashed line in Figure 2A is the one to one line where points would fall if the charge neutralization substitutions had exactly the same effect on stability as the alanine substitutions at these sites. If the alanine and charge neutralization substitutions are equivalent in their effects, the simplest interpretation is that the packing, van der Waals, or hydrogen-bonding interactions are not contributing significantly to the stability of the protein and that the electrostatic interactions of the ionized group predominate in the energetics of the wild-type protein at this site. In

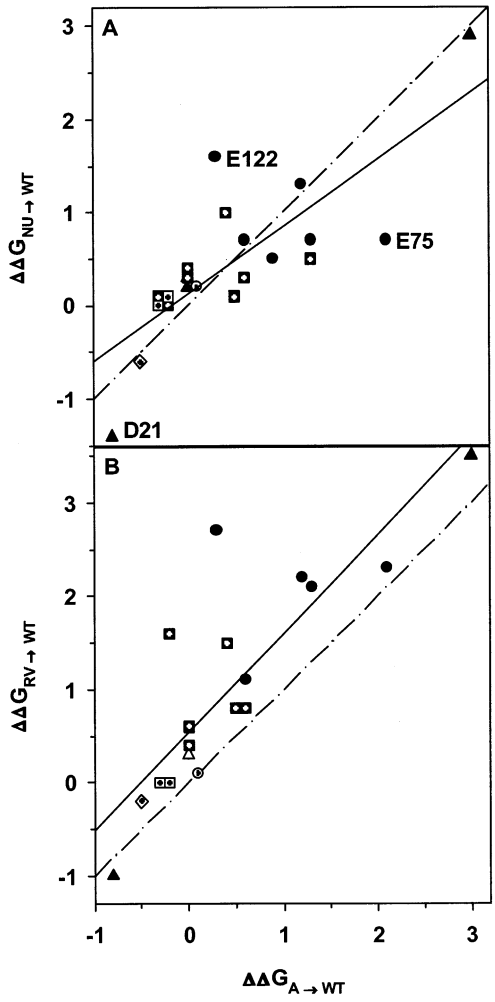

FIGURE 2: Change in stability of charge neutralization or charge reversal substitution versus change in stability of alanine substitution at the same site. Glutamic, aspartic, histidine, and lysine residues in the wild-type protein are identified with circles, triangles, diamond, and squares, respectively. Filled symbols indicate residues that are involved in hydrogen-bonding and/or ionic interactions in the wild-type protein; unfilled symbols are used for the remainder. A filled dot in a hollow symbol or a hollow dot in filled symbol indicates a relative fractional solvent-accessible surface area of 0.5 or greater. Specific sites discussed in the text are labeled on the appropriate panel(s). (A) Change in stability of charge neutralization substitutions versus change in stability of alanine substitutions. The solid line is the linear least-squares regression line ($r = 0.7901$). The dashed line is the one to one line as discussed in the text. (B) Change in stability of charge reversal substitutions versus change in stability of alanine substitutions. The solid line is the linear least-squares regression line ($r = 0.8446$). The dashed line is the one to one line as discussed in the text.

general, this is exactly the behavior most of these sites show. The effects on stability of alanine and charge neutralization substitutions are fairly similar, with most positions falling close to the one to one line.

Of course, few points are precisely on the line and a few are rather far off of it. In cases where the alanine substitutions are less stable than the charge neutralization substitutions (i.e., data points falling in the lower right quadrant of Figure 2A), the simplest interpretation is that some favorable packing, van der Waals, or hydrogen-bonding interactions are occurring at this site in the wild-type protein that are lost when the side chain is truncated. An example of this may be at E75 where the alanine substitution is much more destabilizing than the glutamine substitution. The side chain of the wild-type glutamate residue at site 75 interacts with the side chain of the lysine residue at site 9 (*27*, *49*). This perhaps indicates that there are some stabilizing van der Waals interactions that are removed when this site is substituted to alanine. The case of D21 is another example where both the D21A and D21N mutations are stabilizing, an unusual occurrence. This aspartate is a highly conserved residue in the active site but is in close proximity to a number of other negatively charged residues and is somewhat buried. Removing the charge of D21 is stabilizing, but truncating the side chain must remove some other favorable interaction since the alanine substitution is not as stabilizing as the asparagine substitution at site 21.

One interpretation of the case in which the alanine substitution is more stable than the charge neutralization substitution (i.e., data points falling in the upper left quadrant of Figure 2A) is that the site has destabilizing steric interactions counterbalanced by favorable electrostatic interactions of the wild-type side chain. This may be the case at site 122. The side chain of the wild-type glutamate residue at site 122 interacts with the side chains of K116 and R126 (*49*). The E122Q mutation is much more destabilizing than the alanine substitution.

We emphasize that such behavior is the exception rather than the rule. Most of these sites show remarkable correspondence in the effects of the alanine and the charge neutralization substitutions. Since these two substitutions are similar in that they remove the potential for ionic interactions, but differ markedly in other potential interactions, it seems evident that the observed energetic effects are dominated by electrostatic interactions.

This conclusion is reinforced strongly by the comparison of effects of charge reversal and alanine substitutions shown in Figure 2B. Again, the dashed line in Figure 2B is the one to one line where points would fall if the charge reversal substitutions had exactly the same effect on stability as the alanine substitutions at these sites. Obviously the effects of the alanine substitutions are well correlated with the effects of the charge reversal mutation, with the regression line having a slope of almost exactly one.

What is striking about Figure 2B is that virtually every point lies above the one to one line, falling in the upper left quadrant. In other words, in nearly every case, the alanine substitution is more stable than the charge reversal substitution. This is precisely what one would expect if electrostatic interactions dominate the energetics of these mutations. Reversing the charge should reverse the sign of the energetic contribution. Most of the charges appear to be in net stabilizing environments, and reversing the charge is much more destabilizing than merely removing it as the alanine mutation does.

A direct comparison of the charge reversal and neutralization mutations is also useful. This is shown in Figure 3. If Coulombic interactions dominate, the energetic effects of a charge reversal substitution would be expected to have twice the effect of simply neutralizing the charge. In fact, the average loss of stability for charge reversal is 1.0 kcal/mol with a standard deviation of 1.1 kcal/mol. Charge neutralization mutations average a stability loss of only 0.5 ± 0.8 kcal/mol. Of course, direct comparison of the two mutations at any given individual site does not necessarily give a two to

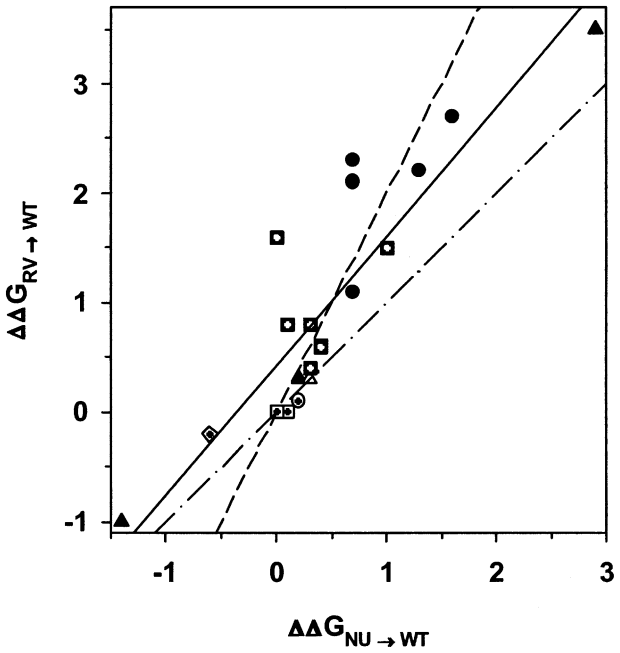

FIGURE 3: Change in stability of charge neutralization substitutions versus change in stability of charge reversal substitutions. All circles are glutamates in the wild-type protein. Glutamic, aspartic, histidine, and lysine residues in the wild-type protein are identified with circles, triangles, diamond, and squares, respectively. Filled symbols indicate residues that are involved in hydrogen-bonding and/or ionic interactions in the wild-type protein. A filled dot in a hollow symbol or a hollow dot in filled symbol indicates a relative fractional solvent-accessible surface area of 0.5 or greater. The solid line is the linear least-squares regression line ($r = 0.8857$). The dashed line is the one to one line as discussed in the text. The dotted line is the two to one line as discussed in the text.

one ratio. The correspondence should not be perfect since the protein has the ability to accommodate the mutation by reorienting the substituted side chain in some way so as to avoid any unfavorable electrostatic interactions caused by reversing the charge at these sites. Further, the reversal of charge mutation necessarily alters the length of the side chain, and this moves the charge toward or further away from the protein surface. However, when the effects are plotted against one another (Figure 3), it is remarkable how many points fall near the two to one line shown for reference.

The results discussed above demonstrate that overall the charge neutralization and the alanine substitutions destabilize the protein to approximately the same extent and that the charge reversal substitutions are almost twice as destabilizing as the charge neutralization substitutions. This clearly and unequivocally indicates that, on average, electrostatic interactions dominate the energetic effects of mutating these ionizable residues. This contradicts the conclusions drawn in an earlier study (*19)* where it was concluded that the ionizable residues in nuclease contributed to the stability of the protein primarily through packing interactions and not through interactions that depended on the charge of the side chains. This earlier conclusion is clearly incorrect.

However, this should not be taken to imply that packing interactions on the surface are unimportant. The mutations made in the current study were chosen deliberately to minimize packing disruptions. Indeed, a study of phenylalanine substitutions at many of the same sites on the surface of staphylococcal nuclease, a much greater change in residue size and shape, concluded that optimizing the packing on the surface of the protein was important to the stability of nuclease (*20*). The work presented here does not contradict that conclusion but does add to it the certainty that the electrostatic interactions of the charged groups are important as well and are, on average, stabilizing.

The phrase "on average" is a key qualifier to note. Much of the confusion in the literature about the importance of electrostatic interactions may be because relatively few interactions have been systematically examined in any one protein. As the results presented here show, a wide range of effects is possible. Neutralizing the charge in the D77N mutation costs 2.7 kcal/mol, and reversing it in D77K causes the rather breathtaking loss of 3.5 kcal/mol. On the other hand, as already noted earlier, D21N and D21K stabilize the protein by 1.2 and 1.0 kcal/mol, respectively. Rational design and modification of protein structure and stability will require accurate prediction of electrostatic effects. Some of the causes for this range of effects are obvious. For example, even a cursory examination of Table 2 shows that the more solvent exposed a residue is, the less the energetic effects upon mutation. It would seem obvious that involvement of a residue in an ionic interaction should affect energetics as well, but an examination of Figure 2 shows that when defined by simple distance criteria the presence or absence of such interactions does not seem to correlate well with the magnitude of the observed effects.

Clearly, a more sophisticated approach for evaluating the electrostatic consequences of mutation of ionizable residues is necessary, and many methods for calculation of electrostatic energies have been detailed in the literature. We used the FDPB method to assess structurally the consequences of charge reversal or neutralization (*29*). This method was chosen, despite the inherent limitations of continuum methods, because empirical modifications have greatly increased its capacity to reproduce pK_a values and the magnitude of interaction energies between individual pairs of charges. This method works particularly well in the case of surface residues in staphylococcal nuclease, as has been recently demonstrated (*9*, *10*).

The results of the FDPD calculations are given in Tables 3 and 4. The critical test, the agreement between calculation and experiment, is shown in Figure 4. In panel A the experimentally observed energetic effects for the charge reversal mutations are plotted against the calculated electrostatic effects, in panel B the corresponding comparison is made for the charge neutralization mutations, and in panel C the corresponding comparison is made for the alanine mutations. The agreement between the computed and measured free energies is good, in fact, much better than in some other studies comparing experiment and theory (*11*, *12*, 19, 52, 53). The FDPB method reproduces the magnitude of the shift in stability well. The direction of the shift (i.e., whether the mutant is stabilizing or destabilizing) is calculated correctly for almost all of the mutants. This is encouraging in two respects. First, the calculations *only* take into account electrostatic effects. van der Waals interactions, hydrophobic effects, and entropic effects are ignored. Consequently, the good agreement is further evidence that our conclusion that the effects of these mutations are dominated by electrostatic interactions is correct. Second, the agreement is an indication that our ability to predict electrostatic effects accurately is fairly good. However, few points are precisely on the one

Table 4: Contributions by the Charge−Dipole Background, Born Energy, and Charge−Charge Energies to the Calculated $\Delta\Delta G_{elec}$ for the Alanine, Charge Neutralization, and Charge Reversal Substitutions

	Ala			RV			NU		
residue	G_{bg}[a]	G_{Born}[b]	G_{ij}[c]	G_{bg}[a]	G_{Born}[b]	G_{ij}[c]	G_{bg}[a]	G_{Born}[b]	G_{ij}[c]
E10	−0.69	1.14	−1.05	−0.64	0.93	−1.66	−0.46	1.06	−1.09
D19	−2.08	1.81	0.63	−2.28	0.73	0.52	−1.86	1.72	0.56
D21	−0.69	2.00	0.27	−1.20	0.09	1.59	−0.70	1.46	0.17
K28	−0.08	0.30	−0.33	−0.01	−0.22	−0.69	−0.26	0.25	−0.36
K48	0.00	0.03	0.16	0.16	−0.13	0.42	−0.02	0.01	0.13
E57	−0.90	0.58	−0.48	−0.97	0.50	−0.88	−0.73	0.54	−0.45
K63	−0.05	0.61	−1.13	0.13	0.03	−1.74	0.03	0.48	−1.10
K64	−0.36	0.10	0.07	−0.71	−0.04	−0.01	−0.38	0.11	0.05
E67	−0.07	0.95	−2.10	0.06	0.76	−3.01	−0.08	0.72	−2.10
K70	−0.18	0.23	0.11	−0.13	0.04	−0.18	−0.13	0.13	0.06
E73	−0.63	0.88	−0.49	−1.18	0.23	−1.26	−0.55	0.85	−0.48
E75	−1.41	1.73	−0.90	−1.69	0.24	−1.91	−1.77	1.60	−0.84
D77	−1.88	2.01	−0.56	−2.35	0.45	−2.43	−1.77	2.01	−0.57
K78	0.27	0.46	−0.23	−0.03	−0.27	−1.25	0.05	0.37	−0.29
K84	0.85	0.54	−0.26	1.37	0.20	−0.54	0.74	0.51	−0.25
K97	−0.15	0.18	−0.33	−0.27	−0.11	−0.75	−0.18	0.17	−0.33
E122	−0.08	1.05	−1.82	0.17	0.00	−3.23	−0.56	0.96	−1.75
H124	0.00	0.27	−0.05	0.33	−0.27	0.01	−0.24	0.17	−0.04
K127	0.17	0.06	0.30	0.42	−0.46	0.60	0.15	0.05	0.25
K133	−0.18	1.10	−1.28	−0.48	0.28	−1.70	−0.60	0.99	−1.25
E135	−0.07	0.81	−2.02	0.08	0.72	−2.61	0.06	0.76	−1.88

[a] The background terms (G_{bg}) contain contributions from Coulombic interactions between the charged group of interest and permanent dipoles in the protein. [b] The Born energy (G_{Born}) terms describe the change in hydration upon transfer of the ionizable group of interest from water to the protein site. [c] The charge−charge terms (G_{ij}) describe the contributions from Coulombic interactions between the ionizable group of interest with other ionizable residues in the protein.

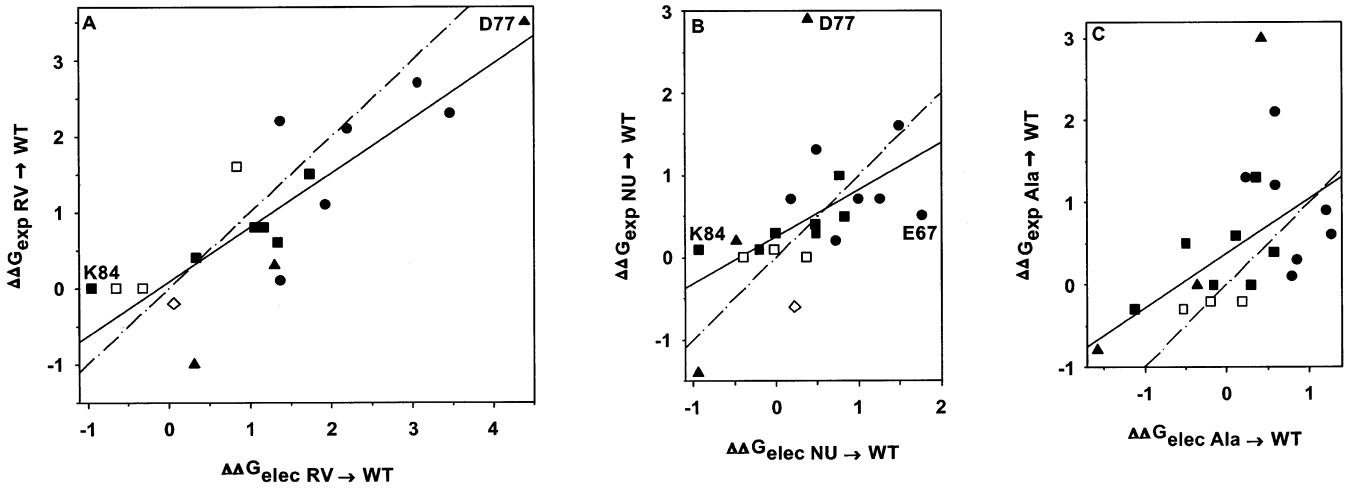

FIGURE 4: Comparison of calculated change in stability due to electrostatic effects with experimentally observed change in stability. Glutamic, aspartic, histidine, and lysine residues in the wild-type protein are identified with circles, triangles, diamond, and squares, respectively. Unfilled symbols indicate residues that are not involved in hydrogen-bonding and/or ionic interactions in the wild-type protein; filled symbols identify those that are. Specific residues discussed in the text are labeled on the appropriate panel(s). (A) Change in stability of the experimentally determined charge reversal substitutions versus change in stability of the calculated charge reversal substitutions. The solid line is the linear least-squares regression line ($r = 0.8497$). The dashed line is the one to one line as discussed in the text. (B) Change in stability of experimentally determined charge neutralization substitutions versus change in stability of the calculated charge neutralization substitutions. The solid line is the linear least-squares regression line ($r = 0.4944$). The dashed line is the one to one line as discussed in the text. (C) Change in stability of experimentally determined alanine substitutions (*19*) versus change in stability of the calculated alanine substitutions. The solid line is the linear least-squares regression line ($r = 0.5209$). The dashed line is the one to one line as discussed in the text.

to one line of perfect correspondence between theory and experiment, and some (e.g., D77 and K84) are quite far off. A closer examination of these disagreements will help to identify avenues for improvement of the calculations. These cases may signal instances where the substitution triggers structural reorganization of the protein that is not captured with the simple energy minimization protocol that was used to model these mutations. Another possibility is that these cases might represent situations where the approximations inherent to the calculations, such as the assumption that the denatured state is devoid of electrostatic interactions or that protein reorganization is quantitatively captured by assuming a protein dielectric of 20, are invalid.

It is important to emphasize that agreement between experiment and calculation is achieved by assuming a relatively high dielectric constant for the interior of the protein. FDPB calculations of electrostatic energy with static structures were performed originally using a low dielectric constant, $\epsilon_{in} = 2-4$, to describe the polarizability of the interior of the protein. Antosiewicz et al. (*11*) showed that,

in the context of the FDPB formalism, the best agreement with experimentally observed energies was obtained in calculations using static structures when the protein interior was treated using a dielectric of 20. The use of a dielectric of 4 exaggerates the calculated electrostatic potentials, leading to large shifts in mutant electrostatic energy, despite the fact that the calculated electrostatic energies represent the balance between Coulombic and hydration effects, which usually have the opposite sign. This is apparently the reason the FDPB calculated energies were found not to be correlated with the alanine substitutions previously (*19*) but are found to be correlated in this study, as shown in Figure 4C.

The good agreement between the calculated and experimental data does not necessarily mean the internal dielectric of the protein is actually 20. Indeed, if ϵ_{in} is increased even further to 40, the correlations with the observed data are increased slightly (data not shown). The largest improvements are obtained for less solvent exposed groups. It has been suggested that lack of conformational sampling in the static structure used in calculations (*12*), relaxation due to the charging process (*54*), and maybe even specific water binding may contribute to the high apparent polarizability. Although the present use of a high dielectric constant works reasonably well, this is clearly an area where further work on improving the computational method is still warranted.

There is some correlation between experimentally determined energies and the degree of solvent exposure. There also appears to be some correlation between the solvent accessibility of a side chain and the accuracy of the calculated energies. For hyperexposed sites, where the fraction of solvent-accessible surface area compared to an exposed reference state is 1.00 or greater, the calculations indicate that the average electrostatic contribution of the side chain to stability is 0.0 kcal/mol. Experimentally, we determined that the average cost in stability of removing the charge at these hyperexposed sites is indeed very small, only 0.2 kcal/mol. The discrepancies between the calculated and the experimental energies are increased at the marginally accessible sites where the fractional solvent-accessible surface area is between 0.09 and 0. The calculations indicate that the average electrostatic contribution of the side chain to stability at the marginally accessible sites is 0.3 kcal/mol. The measured average cost of removing the charge at marginally accessible sites is 0.8 kcal/mol. This greater discrepancy between the calculated and experimental energies may be in part because increasing burial increases the side chain interactions with the protein matrix. Hence, there are more van der Waals and hydrophobic interactions for such residues which are not accounted for in the calculation. In addition, this discrepancy could be explained by the fact that the solvation of less solvent exposed groups needs to be modeled more accurately by capturing the effects of side chain flexibility and backbone dynamics.

The underlying assumption throughout this discussion has been that a large contribution to the energetics of nuclease is due to stabilizing electrostatic interactions in the native state protein. However, any mutation can theoretically affect either the native or the denatured state or both. Much work in the past decade has presented evidence that changes in the denatured state may in some cases have dramatic effects on measured energetics of nuclease and other proteins (*55*, *56*). It might be the case for some of the mutants studied here that the character of the denatured state is different from that of wild type, due to the mutation. As is commonly the case with staphylococcal nuclease mutants (*19*, *20*, *57*, *58*), fairly large changes in the value of m_{GuHCl} are apparent in Table 1. Mutants with significant changes in m_{GuHCl} and C_m values have been conjectured to have changes in the solvent-accessible surface in the denatured state and altered denatured state energetics from wild type (*57*, *58*). Thus, interpretation of the data presented in this paper should not be based on the assumption that the denatured states are equivalent for all of the mutants. In fact, in this study the substitutions with the largest shifts in m_{GuHCl} value from wild type are also among the mutants with the largest shifts in stability.

The computational method used here is restricted by the assumptions made for the denatured state. A model of a noninteracting random coil is implied, where all ionizable residues experience no net electrostatic effects and titrate with the pK_a values obtained from model compounds (*11*, *12*, *28*, *29*). There is experimental evidence of residual electrostatic interactions in nuclease (*59*) and other proteins (*60*, *61*). Some groups have investigated the use of structured or interacting denatured states and have found some improvement in predicted energetics (*62*−*64*). The possibility of residual electrostatic interactions as a reason behind some of the discrepancies between the calculated and measured energies in Figure 4 will have to be explored on a case by case basis. For example, the two largest shifts measured between the observed and the calculated free energies are found for D77 and E67, both of which have among the largest shifts in m_{GuHCl} values. Most of the large discrepancies between observed and calculated $\Delta\Delta G$ values can be associated with change in m_{GuHCl}. Whether this is a complete explanation for the differences is less certain. Both D77 and E67 have interactions with other side chains, and disruption of these contacts may lead to changes in the native as well as the denatured state. Indeed, as discussed earlier, it seems certain that packing interactions are critical for explaining the changes in energetics at position 67. Nevertheless, better modeling of the denatured state is clearly vital for improving the accuracy of calculated energies.

The data in Tables 1−3 show that most surface-ionizable groups in staphylococcal nuclease experience net favorable electrostatic effects. This is consistent with the general observation in many proteins that the pK_a values of surface-ionizable residues are usually shifted in the direction that signals net favorable electrostatic interactions (*65*). This implies that surface-charged groups minimize dehydration and maximize favorable Coulombic interactions with other charged atoms and with permanent dipoles. This prevalence of net favorable electrostatic environments of surface groups can be rationalized in two ways (*66*, *67*). Either the composition and properties of the surfaces of proteins have been tuned throughout evolution to obtain net stabilizing arrangements or the surface-ionizable side chains are endowed with the freedom to organize themselves into net stabilizing environments during the folding reaction to minimize the very high cost of dehydrating charged groups as they are buried in the nascent tertiary fold. The observation that the cost of reversing the polarity of charges is on average more costly than the neutralization of charge suggests that the side chains are not particularly effective at rearranging themselves upon folding, to maximize net favorable elec-

trostatic interactions. This implies that the net favorable electrostatic environments of surface groups are the result of evolutionary fine-tuning of the geometrical disposition of surface side chains. However, compared to other types of noncovalent contributions, the net contributions by surface electrostatics are modest. Therefore, it seems likely that the driving force behind this evolution was solubility as much or more so than stability.

CONCLUSIONS

The results presented here demonstrate conclusively that electrostatic interactions are *the* single most important net stabilizing factor for surface-ionizable residues in staphylococcal nuclease. While packing and hydrophobic interactions are also important for some ionizable residues, electrostatic interactions with the charged group dominate the energetics of these side chains as a whole. Overall, the calculations with continuum methods are in remarkably good agreement with experimental data. The cost of reversing the polarity of a surface charge is approximately twice the cost of neutralizing the charge. These experimental results are consistent with the notion that the tuning of the surfaces of proteins throughout evolution results in the placement of most surface-ionizable groups in net favorable environments. The calculations presented include neither explicit solvation, side chain flexibility, nor salt binding, and they assume a single, equivalent denatured state. It seems likely that it will be possible to predict the consequences of mutations upon electrostatic energetics even more confidently as solutions to these problems become available.

REFERENCES

1. Leung, K. W., Liaw, Y., Chan, S. C., Lo, H. Y., Musayev, F. N., Chen, J. Z. W., Fang, H. J., and Chen, H. M. (2001) Significance of local electrostatic interactions in staphylococcal nuclease studied by site-directed mutagenesis, *J. Biol. Chem. 276*, 46039.
2. Tissot, A. C., Vuilleumier, S., and Fersht, A. R. (1996) Importance of two buried salt bridges in the stability and folding pathway of barnase, *Biochemistry 35*, 6786.
3. Sali, D., Bycroft, M., and Fersht, A. R. (1991) Surface electrostatic interactions contribute little of stability of barnase, *J. Mol. Biol. 220*, 779.
4. Sun, D. P., Sauer, U., Nicholson, H., and Matthews, B. W. (1991) Contributions of engineered surface salt bridges to the stability of T4 lysozyme determined by directed mutagenesis, *Biochemistry 30*, 7142.
5. Blasie, C. A., and Berg, J. M. (1997) Electrostatic interactions across a beta-sheet, *Biochemistry 36*, 6218.
6. Horovitz, A., Serrano, L., Avron, B., Bycroft, M., and Fersht, A. R. (1990) Strength and cooperativity of contributions of surface salt bridges to protein stability, *J. Mol. Biol. 216*, 1031.
7. Loewenthal, R., Sancho, J., Reinikainen T., and Fersht, A. R. (1993) Long-range surface charge−charge interactions in proteins. Comparison of experimental results with calculations from a theoretical method, *J. Mol. Biol. 232*, 574.
8. Serrano, L., Horovitz, A., Avron, B., Bycroft, M., and Fersht, A. R. (1990) Estimating the contribution of engineered surface electrostatic interactions to protein stability by using double-mutant cycles, *Biochemistry 29*, 9343.
9. Lee, K. K., Fitch, C. A., Lecomte, J. T. J., and García-Moreno E, B. (2002) Electrostatic effects in highly charged proteins: salt sensitivity of pK_a values of histidines in staphylococcal nuclease, *Biochemistry 41*, 5656.
10. Lee, K. K., Fitch, C. A., and García-Moreno E, B. (2002) Distance dependence and salt sensitivity of pairwise, Coulombic interactions in a protein, *Protein Sci. 11*, 1004.
11. Antosiewicz, J., McCammon, J. A., and Gilson, M. K. (1994) Prediction of pH-dependent properties of proteins, *J. Mol. Biol. 238*, 415.
12. Antosiewicz, J., McCammon, J. A., and Gilson, M. K. (1996) The determinants of pK_as in proteins, *Biochemistry 35*, 7819.
13. García-Moreno E., B., Chen, L. X., March, K. L., Gurd, R. S., and Gurd, F. R. N. (1985) Electrostatic interactions in sperm whale myoglobin. Site specificity, roles in structural elements, and external electrostatic potential distributions, *J. Biol. Chem. 260*, 14070.
14. Ramos, C. H., Kay, M. S., and Baldwin, R. L. (1999) Putative interhelix ion pairs involved in the stability of myoglobin, *Biochemistry 38*, 9783.
15. van Vlijmen, H. W. T., Schaefer, M., and Karplus, M. (1998) Improving the accuracy of protein pK_a calculations: conformational averaging versus the average structure, *Proteins 33*, 145.
16. Grimsley, G., Shaw, K., Fee, L., Alston, R., Huyghues-Despointes, B., Thurlkill, R., Scholtz, J., and Pace, C. (1999) Increasing protein stability by altering long-range coulombic interactions, *Protein Sci. 8*, 1843.
17. Loladze, V., Ibarra-Molero, B., Sanchez-Ruiz, J., and Makhatadze, G. (1999) Engineering a thermostable protein via optimization of charge−charge interactions on the protein surface, *Biochemistry 38*, 16419.
18. Spector, S., Wang, M., Carp, S., Robblee, J., Hendsch, Z., Fairman, R., Tidor, B., and Raleigh, D. (2000) Rational modification of protein stability by the mutation of charged surface residues, *Biochemistry 39*, 872.
19. Meeker, A. K., García-Moreno, B. E., and Shortle, D. (1996) Contributions of the ionizable amino acids to the stability of staphylococcal nuclease, *Biochemistry 35*, 6443.
20. Schwehm, J. M., Kristyanne, K. S., Biggers, C. C., and Stites, W. E. (1998) Stability effects of increasing the hydrophobicity of solvent-exposed side chains in staphylococcal nuclease, *Biochemistry 37*, 6939.
21. Sun, D. P., Soderlind, E., Baase, W. A., Wozniak, J. A., Sauer, U., Matthews, B. W. (1991) Cumulative site-directed charge-change replacements in bacteriophage T4 lysozyme suggest that long-range electrostatic interactions contribute little to protein stability, *J. Mol. Biol. 221*, 873.
22. Takano, K., Tsuchimori, K., Yamagata, Y., and Yutani, K. (2000) Contribution of salt bridges near the surface of a protein to the conformational stability, *Biochemistry 39*, 12375.
23. Kunkel, T. A. (1985) Rapid and efficient site-specific mutagenesis without phenotypic selection, *Proc. Natl. Acad. Sci. U.S.A. 82*, 488.
24. Kunkel, T. A., Roberts, J. D., and Zakour, R. A. (1987) Rapid and efficient site-specific mutagenesis without phenotypic selection, *Methods Enzymol. 154*, 367.
25. Stites, W. E., Byrne, M. P., Aviv, J. Kaplan, M., and Curtis, P. M. (1995) Instrumentation for automated determination of protein stability, *Anal. Biochem. 227*, 112.
26. Schwehm, J. M., and Stites, W. E. (1998) Application of automated methods for determination of protein conformational stability, *Methods Enzymol. 295*, 150.
27. Hynes, T. R., and Fox, R. O. (1991) The crystal structure of staphylococcal nuclease refined at 1.7 A resolution, *Proteins: Struct., Funct., Genet. 10*, 92.
28. Gilson, M. K. (1995) Theory of electrostatic interactions in macromolecules, *Curr. Opin. Struct. Biol. 5*, 216.
29. Madura, J. D., Briggs, J. M., Wade, R. C., Davis, M. E., Luty, B. A., Ilin, A., Antosiewicz, J., Gilson, M. K., Bagheri, B., Scott, L. R., and McCammon, J. A. (1995) Electrostatics and diffusion of molecules in solution: simulations with the University of Houston brownian dynamics program, *Comput. Phys. Commun. 91*, 57.
30. Jorgensen, W. L., and Tirado-Rives, J. (1988) The OPLS [optimized potentials for liquid simulations] potential functions for proteins, energy minimizations for crystals of cyclic peptides and crambin, *J. Am. Chem. Soc. 110*, 1657.
31. Lee, B., and Richards, F. M. (1971) The interpretation of protein structures: estimation of static accessibility, *J. Mol. Biol. 55*, 379.
32. Stites, W. E., Gittis, A. G., Lattman, E. E., and Shortle, D. (1991) In a staphylococcal nuclease mutant the side-chain of a lysine replacing valine 66 is fully buried in the hydrophobic core, *J. Mol. Biol. 221*, 7.
33. Dwyer, J. J., Gittis, A. G., Karp, D. A., Lattman, E. E., Spencer, D. S., Stites, W. E., and Garcia-Moreno, E. B. (2000) High apparent dielectric constants in the interior of a protein reflect water penetration, *Biophys. J. 79*, 1610.
34. Mayr, L. M., and Schmid, F. X. (1993) Stabilization of a protein by guanidinium chloride, *Biochemistry 32*, 7994.

35. Monera, O. D., Kay, C. M., and Hodges, R. S. (1994) Protein denaturation with guanidine hydrochloride or urea provides a different estimate of stability depending on the contributions of electrostatic interactions, *Protein Sci. 3*, 1984.
36. Gianni, S., Brunori, M., and Travaglini-Allocatelli, C. (2001) Refolding kinetics of cytochrome *c*(551) reveals a mechanistic difference between urea and guanidine, *Protein Sci. 10*, 1685.
37. Del Vecchio, P., Graziano, G., Granata, V., Barone, G., Mandrich, L., Manco, G., and Rossi, M. (2002) Temperature- and denaturant-induced unfolding of two thermophilic esterases, *Biochemistry 41*, 1364.
38. Akhtar, M. S., Ahmad, A., and Bhakuni, V. (2002) Guanidinium chloride- and urea-induced unfolding of the dimeric enzyme glucose oxidase, *Biochemistry 41*, 3819.
39. Cobos, E. S., Filimonov, V. V., Galvez, A., Valdivia, E., Maqueda, M., Martinez, J. C., and Mateo, P. L. (2002) The denaturation of circular enterocin AS-48 by urea and guanidinium hydrochloride, *Biochim. Biophys. Acta 1598*, 98.
40. Ibarra-Molero, B., Loladze, V. V., Makhatadze, G. I., and Sanchez-Ruiz, J. M. (1999) Thermal versus guanidine-induced unfolding of ubiquitin. An analysis in terms of the contributions from charge−charge interactions to protein stability, *Biochemistry 38*, 8138.
41. Smith, J. S., and Scholtz, J. M. (1996) Guanidine hydrochloride unfolding of peptide helices: separation of denaturant and salt effects, *Biochemistry 35*, 7292.
42. Gupta, R., Yadav, S., and Ahmad, F. (1996) Protein stability: urea-induced versus guanidine-induced unfolding of metmyoglobin, *Biochemistry 35*, 11925.
43. Gokhale, R. S., Ray, S. S., Balaram, H., and Balaram, P. (1999) Unfolding of Plasmodium falciparum triosephosphate isomerase in urea and guanidinium chloride: evidence for a novel disulfide exchange reaction in a covalently cross-linked mutant, *Biochemistry 38*, 423.
44. Guidry, J. J., Moczygemba, C. K., Steede, N. K., Landry, S. J., and Wittung-Stafshede, P. (2000) Reversible denaturation of oligomeric human chaperonin 10: denatured state depends on chemical denaturant, *Protein Sci. 9*, 2109.
45. Hornby, J. A., Luo, J. K., Stevens, J. M., Wallace, L. A., Kaplan, W., Armstrong, R. N., and Dirr, H. W. (2000) Equilibrium folding of dimeric class mu glutathione transferases involves a stable monomeric intermediate, *Biochemistry 39*, 12336.
46. Hung, H. C., and Chang, G. G. (2001) Multiple unfolding intermediates of human placental alkaline phosphatase in equilibrium urea denaturation, *Biophys. J. 81*, 3456.
47. Russell, B. S., and Bren, K. L. (2002) Denaturant dependence of equilibrium unfolding intermediates and denatured state structure of horse ferricytochrome *c*, *J. Biol. Inorg. Chem. 7*, 909.
48. Kabsch, W., and Saunders, C. (1983) Dictionary of protein secondary structure: pattern recognition of hydrogen-bonded and geometrical features, *Biopolymers 22*, 2577.
49. Chen, J., Lu, Z., Sakon, J., and Stites, W. E. (2000) Increasing the thermostability of staphylococcal nuclease: implications for the origin of protein thermostability, *J. Mol. Biol. 303*, 125.
50. Vijayakumar, M., and Zhou, H. X. (2001) Salt bridges stabilize the folded structure of barnase, *J. Phys. Chem. B 105*, 7334.
51. Dong, F., and Zhou, H. X. (2002) Electrostatic contributions to T4 lysozyme stability: Solvent-exposed charges versus semi-buried salt bridges, *Biophys. J. 83*, 1341.
52. Kao, Y.-H., Fitch, C. A., Bhattacharya, S., Sarkisian, C. J., Lecomte, T. J. T., and García-Moreno E., B. (2000) Salt effects on ionization equilibria of histidines in myoglobin, *Biophys. J. 79*, 1637.
53. Forsyth, W. R., Gilson, M. K., Antosiewicz, J., Jaren, O. R., and Robertson, A. D. (1998) Theoretical and experimental analysis of ionization equilibria in ovomucoid third domain, *Biochemistry 37*, 8643.
54. Sham, Y. Y., Chu, Z. T., and Warshel, A. (1997) Consistent calculations of pK_a's of ionizable residues in proteins: semi-microscopic and microscopic approaches, *J. Phys. Chem. B 101*, 4458.
55. Shortle, D., and Ackerman, M. S. (2001) Persistence of native-like topology in a denatured protein in 8 M urea, *Science 293*, 487.
56. Pace, C. N., Alston, R. W., and Shaw, K. L. (2000) Charge−charge interactions influence the denatured state ensemble and contribute to protein stability, *Protein Sci. 9*, 1395.
57. Shortle, D. (1995) Staphylococcal nuclease: a showcase of *m*-value effects, *Adv. Protein Chem. 46*, 217.
58. Wrabl, J., and Shortle, D. (1999) A model of the changes in denatured state structure underlying *m* value effects in staphylococcal nuclease, *Nat. Struct. Biol. 6*, 876.
59. Whitten, S. T., and Garcia-Moreno E., B. (2000) pH dependence of stability of staphylococcal nuclease: evidence of substantial electrostatic interactions in the denatured state, *Biochemistry 39*, 14292.
60. Oliveberg, M., Vuilleumier, S., and Fersht, A. R. (1994) Thermodynamic study of the acid denaturation of barnase and its dependence on ionic strength: evidence for residual electrostatic interactions in the acid/thermally denatured state, *Biochemistry 33*, 8826.
61. Zhou, H. X. (2002) Residual electrostatic effects in the unfolded state of the N-terminal domain of L9 can be attributed to nonspecific nonlocal charge−charge interactions, *Biochemistry 41*, 6533.
62. Elcock, A. H. (1999) Realistic modeling of the denatured states of proteins allows accurate calculations of the pH dependence of protein stability, *J. Mol. Biol. 294*, 1051.
63. Schaefer, M., van Vlijmen, H. W., and Karplus, M. (1998) Electrostatic contributions to molecular free energies in solution, *Adv. Protein Chem. 51*, 1.
64. Zhou, H. X. (2002) A Gaussian-chain model for treating residual charge−charge interactions in the unfolded state of proteins, *Proc. Natl. Acad. Sci. U.S.A. 99*, 3569.
65. Forsyth, W. R., Antonsiewicz, J. M., and Robertson, A. D. (2002) Empirical relationships between protein structure and carboxyl pK_a values in proteins, *Proteins 48*, 388.
66. Spassov, V. Z., Karshikoff, A. D., and Ladenstein, R. (1994) Optimization of the electrostatic interactions in proteins of different functional and folding type, *Protein Sci. 3*, 1556.
67. Wada, A., and Nakamura, H. (1981) Nature of the charge distribution in proteins, *Nature 293*, 757.

BI0266434